Journal of Thermal Science Vol.31, No.5 (2022) 1734–1744

https://doi.org/10.1007/s11630-022-1671-0 **Article ID: 1003-2169(2022)05-1734-11**

Characterization of Swirling Inflow Effects on Turbine Performance under Pulsating Flows

DING Zhanming[1*], WANG Cuicui[1], ZHANG Junyue[1], LIU Ying[2], HOU Linlin[1], ZHUGE Weilin[3], ZHANG Yangjun[3]

1. Science and Technology on Diesel Engine Turbocharging Laboratory, China North Engine Research Institute, Tianjin 300400, China
2. Kangyue Technology (Shandong) Co., Ltd, Shouguang, Shandong 262718, China
3. State Key Laboratory of Automotive Safety and Energy, Tsinghua University, Beijing 100084, China

Abstract: The present study focuses on the influence of the swirling flows on flow behaviors and performance of a radial-flow turbocharger turbine under pulsating inflow condition. To characterize the effects of swirling flow, three sets of simulations of the turbine were carried out, which are an unsteady simulation under pulsating swirling inflow, an unsteady simulation under equivalent pulsating uniform inflow, and quasi-steady simulations under uniform inflow. Results proved that swirling flow has a considerable negative influence on turbine instantaneous performance and lead to 2.5% cycle-averaged efficiency reduction under pulsating flow condition. Swirling inflow would lead to significant losses in both the volute and the rotor, while the pulsating inflow leads to higher losses in the rotor and shows little influence on the losses in the volute. The instantaneous efficiency reduction of the turbine could be correlated with the time-varying inlet swirl strength. Under the influence of unsteady inlet swirls, the volute flow field is highly distorted and the free vortex relation is no longer valid. The swirling flow has strong interactions with the wake flow of the volute tongue, leading to additional losses. Relative flow angle at rotor inlet is remarkably reduced and its distribution is significantly distorted. Strong separation flows and passage vortices would appear in the rotor because of the swirling inflow, leading to inferior rotor performance.

Keywords: swirling inflow, pulsating flow, CFD, turbocharger turbine, internal combustion engine

1. Introduction

To cope with the increasingly severe environmental degradation, turbochargers experienced a swift expansion in the internal combustion engine (ICE) industry in the last decade, as it provides the possibility to cut down carbon dioxide emission while maintaining the power performance of ICE. Turbocharger turbine harvests the exhaust energy of ICE and drives the compressor to boost the intake air and enhance the volumetric efficiency. Based on different demands of boost ratio and airflow rate, single-stage and two-stage turbochargers are widely adopted in ICEs. With the development of turbine aerodynamic efficiency, a highly efficient turbine could harvest more energy from the exhaust gas than that required by the compressor, which inspired people to add

Received: Jul 30, 2020 AE: ZUNINO Pietro Corresponding author: DING Zhanming E-mail: dingl25172@163.com

Abbreviations

CFD	Computational fluids dynamics
HPT	High-pressure turbine
ICE	Internal combustion engine
LPT	Low-pressure turbine
MFP	Mass flow parameter
SST	Shear Stress Transport
VR	Velocity ratio

Symbols

C	Absolute velocity/m·s^{-1}
c_p	Specific heat capacity at constant pressure/ J·(kg·K)$^{-1}$
K	Total pressure loss coefficient
L	Loss
M	Torque/N·m
m	Mass flow rate/kg·s^{-1}
p	Pressure/Pa
T	Temperature/K
t	Time/s
U	Blade tip peripheral speed/m·s^{-1}
W	Work/J
β	Relative flow angle/(°)
γ	Ratio of specific heat capacities
η	Efficiency
π	Expansion ratio
θ	Azimuth angle/(°)
ρ	Density/kg·m^{-3}
τ_{87}	Average swirl angle at 0.87R/(°)
ω	Angular velocity/rad·s^{-1}

Subscripts

0	total state
1	LPT inlet
2	LPT volute outlet/ rotor inlet
3	LPT outlet
a	axial
isen	isentropic
r	rotor
v	volute
θ	circumferential

a power turbine downstream to the turbocharger turbine and further utilize the exhaust energy, known as turbocompounding technology. Turbocompounding is considered as one of the most promising waste heat recovery technical solutions for ICEs because of its system simplicity and considerably fuel-saving potential [1]. To conclude, to cut down emissions and improve fuel economy, turbines are increasingly widely adopted in modern ICEs.

In turbocharged and turbo-compounded engines, turbine efficiency has a significant influence on engine performance. Turbines in turbochargers and turbocompounding systems are designed under steady-state and uniform inflow conditions. In the past two decades, intensive researches have been conducted to improve turbine efficiency under ideally steady and uniform inflow conditions. Nevertheless, instead of steady uniform inflow, turbocharger turbines are always subject to pulsating swirling exhaust gases on ICEs. The pulsating flow is a natural result of the frequent opening and closing of the exhaust valves of ICEs. Swirls of the exhaust gases are caused by the exhaust manifold and curved pipes. As ICEs are becoming more and more compact, the traveling distances of swirls in exhaust systems become shorter and their influence on turbines would become stronger. Both the pulsating and swirling inflows have remarkable effects on turbine efficiency, which have been key obstacles in the path of improving the efficiency of turbocharged and turbo-compounded engines.

Baines [2] reviewed the studies before 2010 concerning turbocharger turbine pulsating flow performance. Relevant experimental studies at the early stage such as Refs. [3, 4] suffered from the lack of test facilities to measure the time-resolved mass flow rate and power of the turbine. Recent unsteady turbine experimental studies as that published by Rajoo et al. [5, 6] and Marelli et al. [7] were conducted on more advanced test facilities. As their test results showed, the turbine exhibits various hysteretic performance characteristics under different pulsating flow conditions. Under pulsating flow conditions, the wave-action effect, which is the continuous interaction of the incoming pulses and the reflected pulses, coexists with the filling-and-emptying effect, which is the effect caused by the flow entering and leaving the turbine at the same time but at different rates. Either wave action or filling-and-emptying could be the dominating effect on turbine performance, depending on the frequency and amplitude of the inlet pulses. The average efficiency under pulsatile flow conditions may considerably deviate from that evaluated through steady and quasi-steady methods [6].

Three-dimensional (3D) computational fluid dynamics (CFD) analysis is extensively used to characterize the flow phenomena and loss mechanisms under pulse flow

conditions. In a CFD investigation, Padzillah et al. [8] examined the turbine performance under different pulse frequencies and turbine speeds, and the authors found that the incidence angle is one of the key parameters influencing turbine efficiency. According to the research conducted by Cao et al. [9], the temporal pressure gradient plays a vital role in the unsteady effects on turbine performance under pulse flow conditions. The CFD analysis of a variable nozzle turbine conducted by Qi et al. [10] shed light on how the inlet pulsation flow propagates in the turbine. According to their study, the pulse amplitude damped by two-thirds in the nozzle. The inlet pulse showed a strong effect on the clearance leakage and shock wave, resulting in considerable flow losses. Through numerical simulation of a twin-entry turbine, Cerdoun and Ghenaiet [11] found that Dean vortices may be generated in the volute under pulse flow conditions and caused non-uniformities at rotor inlet both spanwisely and circumferentially. Xue et al. [12] found that the turbine flow structure and performance are related to the Strouhal number, which indicates the flow unsteadiness. Zhao et al. [13] and Liu et al. [14] introduced methods to improve turbine performance under pulsating flows.

The aforementioned researches about turbine pulsating flow performance had, or more exactly, assumed to have uniform inflow conditions; the influence of swirling flow on turbine pulsating flow performance was not considered. Swirling flow plays a key role in turbine on-engine performance as it is impossible to avoid swirls at the turbine inlet. Long straight pipes are widely used in front of the turbine in test facilities to weaken the swirls, which is not an option in ICE applications due to the system volume limit. Inlet swirls may have a remarkable influence on turbine performance, and neglecting their effects may lead to significant misunderstandings of turbine behaviors.

Only a few studies concern about the swirling inflow effect on the performance of turbocharger turbines. Through a simulation study, Hellstrom and Fuchs [15] found that different types of inlet swirls could significantly weaken the ability of the turbine to utilize exhaust energy under steady-state. Numerous experimental and simulation studies have proved that swirling inflow effects are very significant for turbine performance in two-stage turbocharged and turbo-compounded ICEs. The investigations conducted by Westin and Burenius [16], Zhao et al. [17], and Liu et al. [18, 19] showed that the swirls generated by the high-pressure turbine (HPT) could lead to a 6%–8% efficiency reduction of the low-pressure turbine (LPT) under steady-state.

A few researchers have concerned about turbine behaviors under pulsating swirling conditions. Hellstrom and Fuchs [20] found that manifolds upstream of the turbine have a strong effect on the turbine flow field under pulsating flow conditions, but the authors did not try to separate the effect of the pulsating inflow and the inlet swirling flow. In an experimental study, Kalpakli et al. [21] found that the hysteresis loop of turbine swallowing capacity under pulse flow conditions was significantly damped when a bent pipe is installed upstream to it generating Dean vortices. However, the physics behind the effect was not investigated and the effect of Dean swirls on turbine efficiency was not studied. Lim et al. [22] studied the influence of exhaust manifold on the heat transfer and performance of a turbocharger turbine under pulse flow conditions. They found that the manifold affects the heat transfer and aerodynamic losses in the turbine scroll and rotor significantly.

To summarize, realistic working environments for turbocharger turbines and power turbines on ICEs involve pulsating and swirling inflow, which are two of the most important factors at play that caused the degradations of turbine on-engine performance in comparison with the map performance. While turbine pulsating flow performance has attracted extensive studies, the swirling inflow effect still lacks attention. The authors have published findings of the swirling flow effect on steady turbine performance [23] and compared the swirling inflow effect on turbine steady and pulsating flow performance [24]. In this paper, turbine behaviors under pulsating swirling inflow condition would be characterized with particular concerns about the swirling inflow effect on turbine unsteady flow behaviors. Flow structures and the mechanisms lying behind would be analyzed and discussed.

2. Methodology

A variety of complicated swirls could be generated by exhaust manifolds and bend pipes under pulse flow conditions, which have diverse effects on turbine performance. To establish a fundamental understanding of the swirling flow effect on turbine performance under pulsating flow conditions, bulk swirls with single swirl cores generated by an HPT were considered in this study. The examined turbine serves as the LPT in a two-stage regulated turbocharger in a heavy-duty diesel engine. Although its performance is not considered, the HPT is included in this study as a bulk swirl generator. The main geometry parameters of the HPT and LPT are listed in Table 1.

The effect of inlet swirls on turbine performance under pulsating flow condition could be assessed by comparing turbine performance under pulsating swirling and corresponding pulsating uniform inflow conditions which

have the same inlet mass flow rate and total temperature. To characterize the pulsating and swirling inflow effect, the numerical calculations consist of three steps:

(1) In the first step, the whole two-stage turbine system under pulsating flow condition was simulated. The fluid domain of the simulation conducted in this step is shown in Fig. 1. By including the LPT and its upstream components in one simulation, the performance of the LPT under realistic pulsating swirling flows could be predicted.

Table 1 Main geometry parameters of the HPT and LPT

	HPT	LPT
Type	Mixed-flow	Radial-flow
A/R at volute tongue	29.6 mm	39.4 mm
Blade number	11	12
Radius of rotor inlet (RMS)	53.6 mm	63.3 mm
Inlet blade height	17.8 mm	17.2 mm
Inlet blade angle	–13.3°	0.8°
Outlet blade angle	–43.6°	–53.4°
Hub radius at rotor exit	17.6 mm	18.6 mm
Tip radius at rotor exit	50.3 mm	53.8 mm

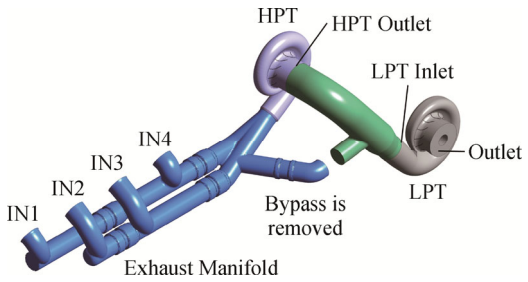

Fig. 1 Fluid domain of the two-stage turbine system

(2) In the second step, the LPT was simulated alone under pulsating uniform inflow condition. To make results comparable, the LPT should be simulated under the same working condition as in step (1) except for the swirls. Therefore, the inlet boundary conditions of LPT in step (2), i.e. the mass flow rate and total temperature, were obtained from simulation results of step (1). The swirling inflow effect could be evaluated by comparing simulation results obtained in steps (1) and (2).

(3) In the last step, the LPT performance was simulated under uniform inflow conditions in a quasi-steady manner. Firstly, a steady performance map of LPT covering the full operating range under pulsating flow conditions was obtained through simulation. Then, based on the pulsating boundary conditions at each time instant, the quasi-steady performance of the turbine was interpolated using the simulated steady performance data.

In all simulations, turbine speeds and outlet static pressure were kept constant. The rotating speeds of the HPT and LPT were 61 927 r/min and 47 815 r/min respectively, which are obtained from one-dimensional engine simulation results. Simulations were carried out using commercial CFD solver ANSYS CFX. Heat transfer was neglected and all the walls were set to be adiabatic. Shear Stress Transport (SST) turbulence model was adopted. For unsteady simulations in steps (1) and (2), the transient rotor-stator method was employed to model the rotor-volute interface, which could account for the transient interactions between the rotor and the volute. The frozen rotor model was used for the steady simulations in step (3). The inlet boundary conditions, grid and time step sensitivity studies of the unsteady simulations in steps (1) and (2) have been reported in Refs. [23, 24]. LPT contains 0.78 and 3.34 million cells in volute and rotor respectively. The y^+ of the LPT wall surfaces is lower than 5 in most parts, which is considered to have sufficient resolution for this investigation. Other parts such as the HPT and exhaust manifold were meshed with similar size. The total cell number of the whole two-stage turbine system shown in Fig. 1 is 9.01 million. The time step for unsteady simulations in steps (1) and (2) was set to be 4.3×10^{-6} s, which equals 1.2 and 1.6 degrees of rotation of the LPT and HPT wheel per time step respectively.

The numerical model is validated by two steady performance tests of LPT, i.e. a flow capacity test and an efficiency test. Two tests were conducted at different sets of turbine speeds. The simulations have the same mass flow rate and total temperature at the turbine inlet as in the tests. As shown in Table 2, the model prediction results are in good agreement with flow capacity and efficiency test results. The largest deviations of predicted expansion ratio and efficiency from test data are within 2%.

Table 2 Comparison of steady test and simulation results of LPT. Simulation models have the same mass flow rate and total temperature at turbine inlet

Rotating Speed/r·min^{-1}	Expansion ratio		Efficiency	
	Test	Simulation	Test	Simulation
40 000	1.52	1.53	–	–
45 000	1.65	1.68	–	–
50 000	1.81	1.85	–	–
55 000	2.06	2.10	74.3%	75.6%
60 000	2.32	2.35	74.3%	74.5%
65 000	2.64	2.66	73.2%	73.0%
70 000	2.96	2.95	71.6%	71.1%
72 000	3.11	3.07	–	–
75 000	–	–	69.9%	68.2%

3. Results and Discussions

3.1 Structure and strength of the swirling flow

In this study, HPT is the predominant source of the swirling flow. Complicated secondary flows generated in the exhaust manifold are shaped into bulk swirls by the HPT. The vortex structures in the two-stage turbine system at the 90° phase angle are visualized by λ_2 criterion [25] in Fig. 2, in which λ_2 is the second eigenvalue of the symmetry square of velocity gradient tensor. Strong bulk swirls generated by the HPT travel downstream into LPT and significantly change the flow structure.

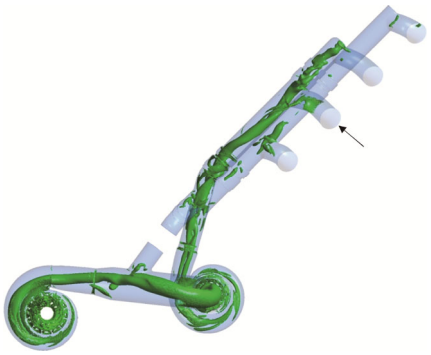

Fig. 2 Vortex structures in the two-stage turbine system at the 90° phase angle

The strength of bulk swirls is evaluated by τ_{87}, as defined in Eq. (1). As proved in a previous study [23], τ_{87} can effectively characterize the strength of bulk swirls and is easy to be measured in experiments.

$$\tau_{87} = \overline{\arctan\left(\frac{C_{\theta,0.87R}}{C_{a,0.87R}}\right)} \tag{1}$$

in which $C_{\theta,0.87R}$ and $C_{a,0.87R}$ are the tangential and axial velocities at 87% radius respectively. τ_{87} represents the average swirl angle at 87% radius.

The variations of τ_{87} at outlet of HPT and inlet of LPT against time are depicted in Fig. 3. Swirling strength at two locations is pulsatile although the rotating speed of HPT is constant since the swirling strength is related to the axial velocity as well. From the HPT outlet to the LPT inlet, swirls travel about six times the diameter of the LPT inlet, and they decay quite significantly in that process. Even though, according to the findings in Ref. [23], swirls at LPT inlet are still strong enough to lead to remarkable turbine performance deterioration. If the connecting pipe of HPT and LPT could be long enough, the swirls at the LPT inlet could be possibly weak enough and their influence on LPT performance may be negligible. However, due to volume restrictions, the distance between HPT and LPT is becoming shorter in most ICE applications, which would enhance the influence of swirling flow on LPT performance. Swirl strength variations at the LPT inlet basically follow the variations at the HPT outlet.

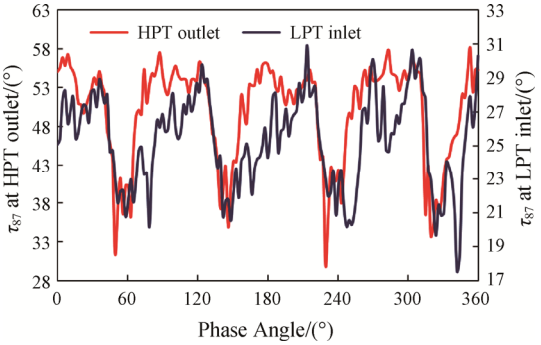

Fig. 3 Comparison of τ_{87} at HPT outlet and LPT inlet

3.2 Swirling flow effect on turbine performance under pulsating flow condition

The effect of swirling flow on the time-resolved and average performance of LPT performance would be discussed in this section. The turbine instantaneous expansion ratio, mass flow parameter (MFP), velocity ratio (VR), and efficiency are calculated by Eqs. (2)–(5) respectively.

$$\pi(t) = \frac{p_{01}(t)}{p_3} \tag{2}$$

$$\mathrm{MFP}(t) = \frac{m_1(t)\sqrt{T_{01}(t)}}{p_{01}(t)} \tag{3}$$

$$VR(t) = \frac{U_2}{\sqrt{2c_p T_{01}(t)\left(1-\pi(t)^{\frac{1-\gamma}{\gamma}}\right)}} \tag{4}$$

$$\eta(t) = \frac{W(t)}{W_{\mathrm{isen},1}(t)} = \frac{M(t)\cdot\omega}{m_1(t)c_p T_{01}(t)\left(1-\pi(t)^{\frac{1-\gamma}{\gamma}}\right)} \tag{5}$$

As expected, the turbine shows hysteretic behaviors under pulsating flow conditions, as shown in Fig. 4, no matter with or without swirling inflow. Swirling inflow leads to a little higher flow capacity and lower efficiency of the turbine under pulse flow conditions. The influence of the inlet swirls on turbine efficiency is especially strong at high velocity ratios that corresponding to low pressure ratios and mass flow rates.

The influence of swirling flow on LPT could be assessed by comparing its performance under pulsating uniform and pulsating swirling conditions, as shown in Eq. (6).

$$\Delta G(t) = G_{\mathrm{pul\&uni}}(t) - G_{\mathrm{pul\&sw}}(t) \tag{6}$$

where G could represent any turbine parameters such as efficiency of the whole turbine and rotor, and rotor inlet flow angles.

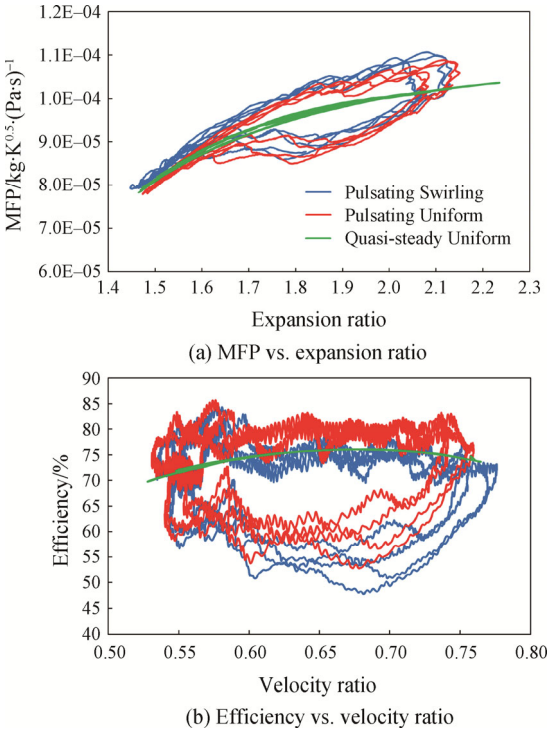

(a) MFP vs. expansion ratio

(b) Efficiency vs. velocity ratio

Fig. 4 Flow capacity and efficiency of LPT

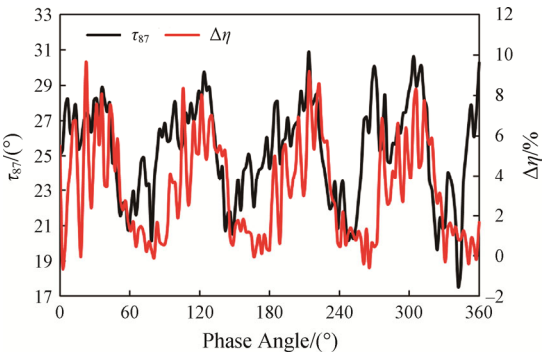

Fig. 5 Variations of τ_{87} at LPT inlet and $\Delta\eta$

Variations of τ_{87} and $\Delta\eta$ are plotted in Fig. 5, from which the correlation between the swirling strength and efficiency reduction could be observed. The efficiency reduction could reach nearly 10% when inlet swirls are strong, and reduce to nearly zero when inlet swirls are weak, which is consistent with the findings under steady-state [23]. A clear time lag between the variations of τ_{87} and $\Delta\eta$ could be noticed, as a natural result of the unsteady effect under pulsating flow conditions.

Turbine aerodynamic losses could be divided into total pressure losses in the volute and aerodynamic losses in the rotor. The total pressure loss coefficient of the volute could be calculated by Eq. (7). Variations of τ_{87} and $-\Delta K_v$ of LPT are plotted in Fig. 6. Swirling inflow leads to significantly higher total pressure loss in turbine volute, and variations of swirling inflow strength lead to a similar variation of total pressure loss of volute with a phase shift. The increase of volute total pressure loss could be explained by stronger secondary flow losses in the volute under swirling inflow conditions.

$$K_v = \frac{p_{01} - p_{02}}{p_{02} - p_2} \tag{7}$$

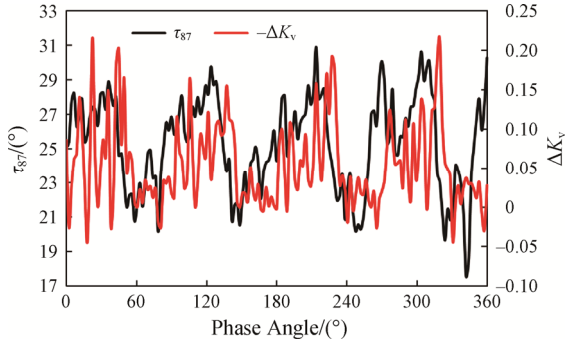

Fig. 6 Variations of τ_{87} at LPT inlet and $-\Delta K_v$

Rotor flow losses increase remarkably under pulsating swirling conditions than pulsating uniform conditions. As discussed in Ref. [23], swirling inflow could lead to a reduction of absolute peripheral velocity at rotor inlet (denoted as $C_{\theta 2}$), hence the relative inlet flow angle of the rotor is significantly reduced and rotor efficiency is affected. The same analysis still stands under pulsating flow conditions, as shown in Fig. 7. Rotor efficiency is defined in Eq. (8). The differences between $C_{\theta 2}$ under pulsating swirling and pulsating uniform conditions are large under strong swirling inflow conditions, which will lead to reduction of β_2. Results show that $\Delta\beta_2$ and $\Delta\eta_r$ between pulsating uniform and pulsating swirling conditions vary with time almost synchronously, indicating that the swirling inflow effects on rotor inlet flow angle and rotor efficiency are closely related. According to the loss theory proposed by Futral et al. [26], the same $\Delta\beta_2$ can lead to a different increase of incidence loss and reduction of efficiency at different turbine operating points, which could illustrate why the same τ_{87} at turbine inlet may lead to different performance reductions at a different operating point.

$$\eta_r(t) = \frac{W(t)}{W_{\text{isen},2}(t)} = \frac{M(t)\cdot\omega}{m_2(t)c_p T_{02}(t)\left[1-\left(\frac{p_3}{p_{02}(t)}\right)^{\frac{\gamma-1}{\gamma}}\right]} \tag{8}$$

In many applications, cycle-averaged turbine MFP and efficiency are most concerned. Cycle-averaged quantities show the overall effect of pulsating and swirling inflow on turbine performance. The cycle-averaged MFP, efficiency, efficiency loss in the volute and rotor are defined by Eqs. (9)–(12) respectively, and they are

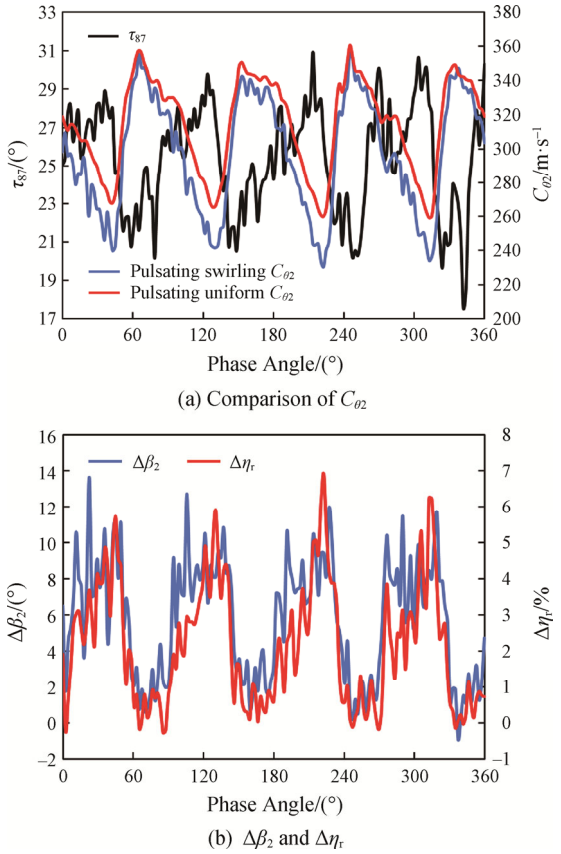

(a) Comparison of $C_{\theta 2}$

(b) $\Delta\beta_2$ and $\Delta\eta_r$

Fig. 7 Variations of $C_{\theta 2}$, $\Delta\beta_2$ and $\Delta\eta_r$

Table 3 Comparisons of the cycle-averaged quantities under pulsating swirling, pulsating uniform, and quasi-steady uniform inflow conditions

	$\overline{\text{MFP}}$ /kg·K$^{0.5}$·(Pa·s)$^{-1}$	$\overline{L}_v$	$\overline{L}_r$	$\overline{\eta}$
Pulsating swirling	9.25×10^{-5}	6.88%	23.4%	69.7%
Pulsating uniform	9.14×10^{-5}	5.54%	22.3%	72.2%
Quasi-steady uniform	9.22×10^{-5}	5.63%	20.8%	73.6%

calculated and listed in Table 3. The pulsating swirling inflow causes a 3.9% reduction of turbine cycle-averaged efficiency compared to equivalent quasi-steady uniform inflow conditions. The pulsating flow alone could lead to a 1.4% efficiency reduction. With the influence of the swirling inflow and the coupling effects of pulsating and swirling inflow, the turbine efficiency was further deteriorated by 2.5%. In comparison with pulsating uniform inflow condition, pulsating swirling inflow caused a 1.3% efficiency loss increment in the volute and 1.1% loss increment in the rotor. Compared with the quasi-steady uniform inflow condition, pulsating uniform inflow caused a 1.5% efficiency loss increment in the rotor and showed little influence on the volute loss. The examined pulsating flow condition appears to have a minor effect on the turbine performance, probably because the pulsating flow condition is near the design point of the LPT and only varies in a small range. Under different pulsating flow conditions, pulsating and swirling inflow may have different influences on turbine efficiency. According to the simulation results under the examined pulsating flow condition, swirling inflow could result in significant losses in both turbine volute and rotor, while pulsating flow may only have a significant effect on losses in the rotor.

$$\overline{\text{MFP}} = \frac{\int_0^T \text{MFP}(t)\,\mathrm{d}t}{T} \tag{9}$$

$$\overline{\eta} = \frac{\int_0^T W(t)\,\mathrm{d}t}{\int_0^T W_{\text{isen},1}(t)\,\mathrm{d}t} \tag{10}$$

$$\overline{L}_v = \frac{\int_0^T W_{\text{isen},1}(t)\,\mathrm{d}t - \int_0^T W_{\text{isen},2}(t)\,\mathrm{d}t}{\int_0^T W_{\text{isen},1}(t)\,\mathrm{d}t}\times 100\% \tag{11}$$

$$\overline{L}_r = \frac{\int_0^T W_{\text{isen},2}(t)\,\mathrm{d}t - \int_0^T W(t)\,\mathrm{d}t}{\int_0^T W_{\text{isen},1}(t)\,\mathrm{d}t}\times 100\% \tag{12}$$

where T refers to the pulse cycle.

3.3 Swirling inflow effect on the volute and rotor flow field

Swirling flow could dramatically alter the flow structure in LPT, which is the root cause of the turbine performance variations. As observed from the fluctuations in Fig. 8, turbine performance deterioration is not a simple function of swirling flow strength at turbine inlet, but influenced by complex flow phenomena. In this section, turbine flow fields under pulsating swirling and pulsating uniform inflow conditions at 270°, 274.5°, 297°, 301.5° and 306° phase angles will be compared and analyzed. As shown in Fig. 8, those five phase angles correspond to local maximum or minimum values of τ_{87} and $\Delta\eta$. Specially, τ_{87} is much higher at 270° than that under 274.5°, but $\Delta\eta$ shows a reverse relation. A similar relation exists between 297° and 301.5°. At 301.5°, τ_{87} is almost the same with that under 306°, but $\Delta\eta$ is only half of that under 306°. Analysing the turbine flow structure under those five phase angles will help understand the flow mechanisms behind the swirling inflow effect.

Fig. 9 gives the pressure distribution at the middle section of volute and mid-span surface of the rotor under pulsating swirling and pulsating uniform conditions at 306° phase angle. Under pulsating swirling inflow condition, the pressure is relatively low in the vortex core region, and the pressure distribution in the volute is distorted remarkably by the swirling inflow, and no

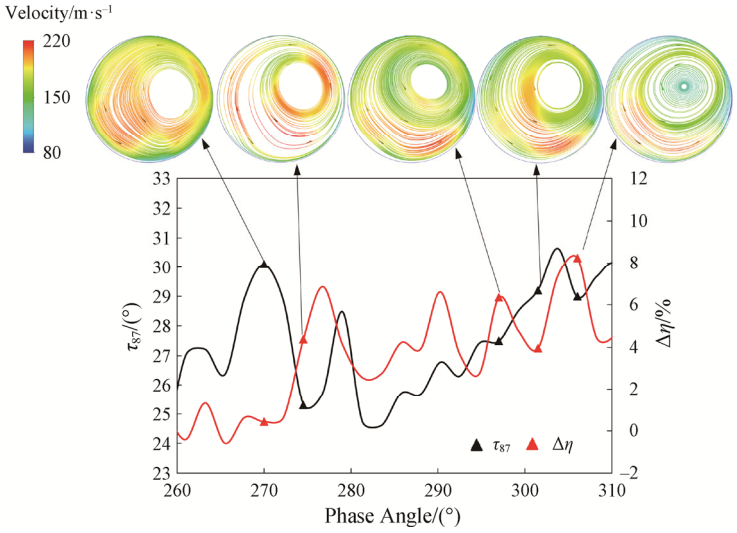

Fig. 8 Variations of τ_{87} at LPT inlet and $\Delta\eta$. Values at 270°, 274.5°, 297°, 301.5° and 306° phase angles are labeled with triangular markers. Surface streamlines at LPT inlet at five phase angles are given.

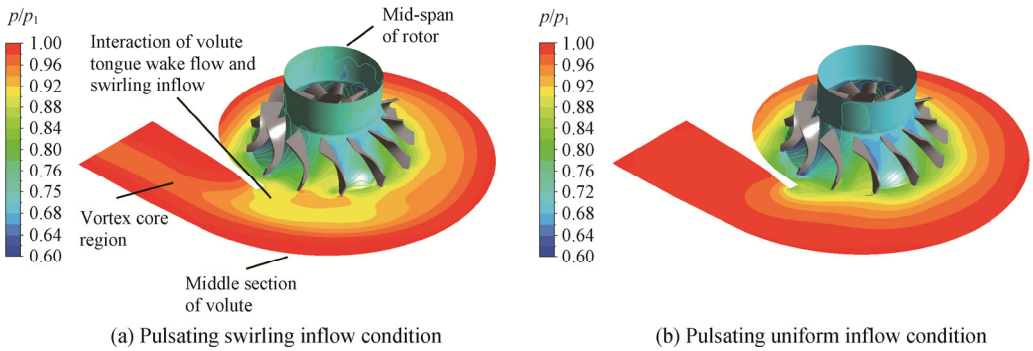

(a) Pulsating swirling inflow condition (b) Pulsating uniform inflow condition

Fig. 9 Pressure distribution at the middle section of the volute and mid-span surface of the rotor under pulsating swirling and pulsating uniform inflow conditions when phase angle is 306°. Pressure is normalized by the inlet static pressure of LPT.

longer decreases uniformly with the radius as in pulsating uniform inflow condition. Distorted pressure distribution would lead to non-uniform performance of rotor passages, which will further lead to turbine performance deterioration. Under pulsating uniform inflow conditions, the wake at the volute tongue has a relatively small influence on the overall pressure distribution. Under pulsating swirling inflow conditions, on the other hand, the incoming vortex has a strong interaction with the wake at the volute tongue and results in a large region of distorted pressure distribution in the volute and corresponding rotor passages. Consequently, more rotor passages would have inferior performance at the volute tongue region due to the vortex-wake interaction.

The distribution of Mach number under pulsating swirling and pulsating uniform inflow conditions at the middle section of the volute and mid-span surface of the rotor is given in Fig. 10. Note that the Mach number in the rotor is calculated using the relative flow velocity. The wake at the volute tongue becomes markedly shorter under pulsating swirling condition than that under pulsating uniform inflow condition. One possible explanation may be that the vortex-wake interaction significantly speeds up the mixing process of high Mach number mainstream flow and low Mach number wake flow. Time lag effect between τ_{87} and $\Delta\eta$ can be understood by comparing the turbine flow field at 270° and 274.5° of the phase angle**.** Swirling strength at LPT inlet is high at 270° but only results in a small reduction of turbine efficiency, because the influence of strong swirls has not affected turbine flow fields yet. On the contrary, although τ_{87} at LPT inlet is relatively smaller at 274.5°, vortex-wake interaction is strong and turbine flow field is significantly distorted because of the swirls that entered the turbine at the previous time; hence turbine efficiency is much more markedly reduced. At phase angle 297°, 301.5° and 306°, the vortex core region is marked by the low Mach number region in the volute, indicating strong swirling inflow effects. Strong vortex in the volute leads to higher loss of $C_{\theta 2}$ under

pulsating swirling than pulsating uniform inflow condition, causing a significant reduction of β_2. The distribution of Mach number is highly distorted both radially and circumferentially especially at phase angle 297° and 306° which may partly explain why the efficiency reduction then is higher than that at 301.5°.

The flow interaction and distortion in the volute would significantly influence the distribution of velocity flow angles at rotor inlet, leading to circumferentially and spanwisely distortion of rotor flow. When the phase angle is 306°, the distribution of β_2 under pulsating swirling and pulsating uniform inflow conditions at the rotor inlet is depicted in Fig. 11. Apart from the tongue region, the β_2 distribution of different rotor passages has a similar pattern under pulsating uniform inflow conditions, while significant differences of the β_2 distribution of different rotor passages could be observed under pulsating swirling inflow conditions. Under the influence of swirling flow, β_2 between 150° to 240° of the azimuth angle is remarkably reduced, which will lead to large incidence loss in the corresponding rotor passages. Besides, the β_2 near the rotor shroud becomes remarkably larger than that near the hub, which would cause large flow separation and strong vortices near the hub. The distortion of β_2 is closely related to the flow distortion in the volute, proving that the flow distortion is one of the key factors behind the swirling inflow effect.

The surface streamlines at the 50% streamwise section of the rotor at 306° phase angle under pulsating swirling and pulsating uniform inflow conditions are depicted in Fig. 12. Under the influence of swirling inflow, strong secondary flows are generated in rotor passages. At about 30° of the azimuth angle, a strong vortex exists due to saparation flow at the upper part of blade suction side.

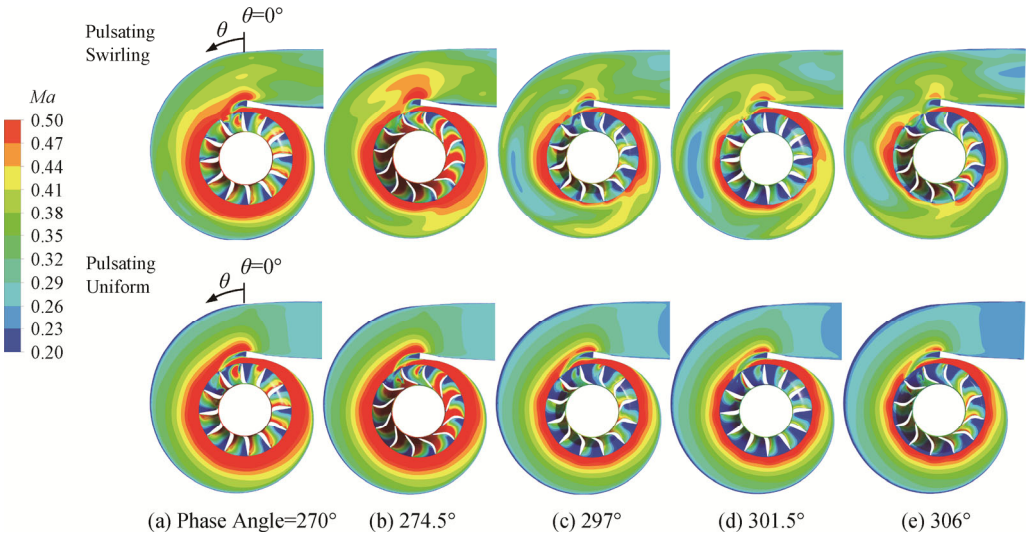

Fig. 10 Distribution of Mach number under pulsating swirling and pulsating uniform inflow conditions at the middle section of the volute and mid-span surface of the rotor

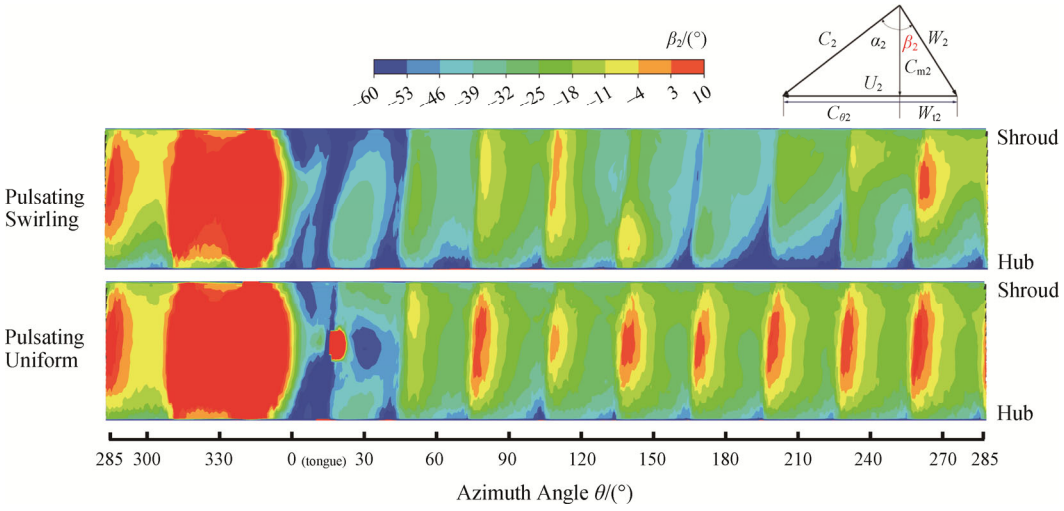

Fig. 11 Distribution of β_2 at 306° phase angle under pulsating swirling and pulsating uniform inflow conditions at the rotor inlet

From 180° to 240° of the azimuth angle, passage vortices and strong secondary flows could be observed under pulsating swirling inflow conditions, resulting in significant increases of rotor losses. The vortices in the rotor are in accordance with the flow distortion in the volute and β_2 distribution at the rotor inlet. Therefore, it can be inferred that the passage vortices are developed from large flow separations at the blade leading edge because of the large relative velocity flow angle.

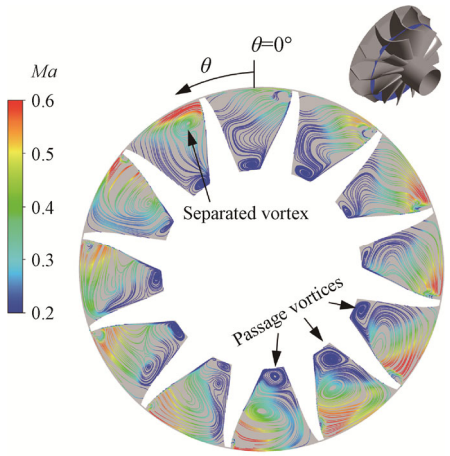

(a) Pulsating swirling inflow condition

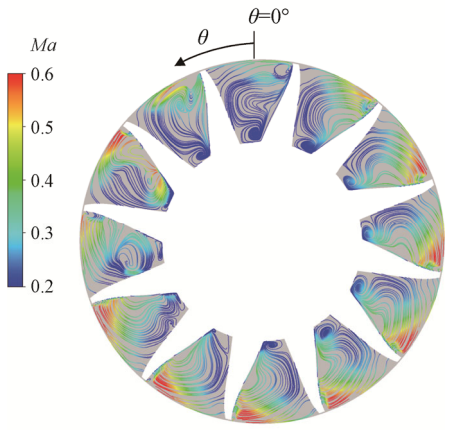

(b) Pulsating uniform inflow condition

Fig. 12 Streamlines at the 50% streamwise section of rotor under pulsating swirling and pulsating uniform inflow conditions when phase angle is 306°

4. Conclusions

In this paper, the swirling inflow effect on turbine performance under pulsating flow condition was characterized by comparing turbine flow behaviors and performance under pulsating swirling, pulsating uniform, and quasi-steady uniform inflow conditions. Results proved that pulsating and swirling inflow are both detrimental to turbine performance, resulting in inferior turbine efficiency under realistic working conditions. The pulsating flow alone caused a 1.4% efficiency reduction. With the influence of the swirling inflow, the turbine efficiency was further deteriorated by 2.5%. Swirling inflow could result in significant losses in both the volute and the rotor, while the pulsating inflow leads to significant losses in the rotor and shows little influence on the volute losses.

The flow distortion and reduction of β_2 are believed to be the two most important factors in the swirling flow effect. Turbine efficiency reduction caused by swirling inflow could be correlated with the swirl strength. Incoming vortices would cause significant flow distortion in the volute, leading to high secondary flow losses and circumferential velocity losses in the volute. Circumferential velocity losses in the volute lead to significant deviation of optimum incidence angle at rotor inlet, resulting in reductions of turbine efficiency. Circumferential and spanwise flow distortion would further deteriorate turbine performance by causing strong vortices and inferior performance of some rotor passages.

Swirling inflow would result in strong vortex-wake interaction at the volute tongue. The circumferential and spanwise distribution of velocity flow angles at the rotor inlet is significantly influenced by the flow interaction and distortion in the volute. Strong separation flows and passage vortices are generated in rotor passages due to reduced relative rotor inlet flow angles and distorted incoming flow; hence rotor performance is exacerbated considerably.

Acknowledgments

The authors would like to thank the foundation of Science and Technology on Diesel Engine Turbocharging Laboratory (No.6142212190101) and Young Elite Scientists Sponsorship Program by CAST (2021QNRC001) for the supports.

References

[1] Aghaali H., Ångström H-E., A review of turbocompounding as a waste heat recovery system for internal combustion engines. Renewable and Sustainable Energy Reviews, 2015, 49: 813–824.

[2] Baines N., Turbocharger turbine pulse flow performance and modelling 25 years on. 9th IMechE International Confererce on Turbochargers and Turbocharging, London, England, 2010, 5: 19–20.
DOI: 10.1243/17547164C0012010028.

[3] Wallace F., Blair G., The pulsating-flow performance of inward radial-flow turbines. ASME 1965 Gas Turbine Conference and Products Show, Washington, 1965, February 28-March 4. DOI: 65-GTP-21.

[4] Dale A., Watson N., Vaneless radial turbocharger turbine performance. IMechE turbocharging and turbochargers,

1986: 65–76.

[5] Rajoo S., Martinez-Botas R., Unsteady effect in a nozzled turbocharger turbine. Journal of Turbomachinery, 2010, 132: 031001.

[6] Rajoo S., Romagnoli A., Martinez-Botas R.F., Unsteady performance analysis of a twin-entry variable geometry turbocharger turbine. Energy, 2012, 38: 176–189.

[7] Marelli S., Capobianco M., Steady and pulsating flow efficiency of a waste-gated turbocharger radial flow turbine for automotive application. Energy, 2011, 36: 459–465.

[8] Padzillah M.H., Rajoo S., Martinez-Botas R.F., Influence of speed and frequency towards the automotive turbocharger turbine performance under pulsating flow conditions. Energy Conversion and Management, 2014, 80: 416–428.

[9] Cao T., Xu L., Yang M., Martinez-Botas R.F., Radial turbine rotor response to pulsating inlet flows. Journal of Turbomachinery, 2014, 136: 071003.

[10] Qi M., Lei X., Wang Z., Ma C., Investigation on the flow characteristics of a VNT turbine under pulsating flow conditions. Proceedings of the Institution of Mechanical Engineers, Part D: Journal of Automobile Engineering, 2017, 233(2): 396–412.

[11] Cerdoun M., Ghenaiet A., Unsteady behaviour of a twin entry radial turbine under engine like inlet flow conditions. Applied Thermal Engineering, 2018, 130: 93–111.

[12] Xue Y., Yang M., Martinez-Botas R.F., Yang B., Deng K., Unsteady performance of a mixed-flow turbine with nozzled twin-entry volute confronted by pulsating incoming flow. Aerospace Science and Technology, 2019, 95: 1–13.

[13] Zhao R.C., Li W.H., Zhuge W.L., Zhang Y.J., Unsteady flow loss mechanism and aerodynamic improvement of two-stage turbine under pulsating conditions. Entropy, 2019, 21(10): 985.

[14] Liu Z., Copeland C., Optimization of a radial turbine for pulsating flows. Journal of Engineering for Gas Turbines and Power, 2020, 142: 051009.

[15] Hellstrom F., Fuchs L., Effects of inlet conditions on the turbine performance of a radial turbine. ASME Turbo Expo 2008: Power for Land, Sea, and Air, Berlin, 2008, 6: 9–13. DOI: GT2008-51088.

[16] Westin F., Burenius R., Measurement of interstage losses of a twostage turbocharger system in a turbocharger test rig. SAE Paper 2010-01-1221.
DOI: 10.4271/2010-01-1221.

[17] Zhao R., Zhuge W., Zheng X., Zhang Y., Yin Y., Li Z., Design of counter-rotating turbine to improve the off-design performance of turbo-compounding systems. ASME Turbo Expo 2013: Turbine Technical Conference and Exposition: American Society of Mechanical Engineers, San Antonio, 2013, 7: 3–7.
DOI: GT2013-94412.

[18] Liu Y., Zhuge W., Zheng X., Zhang Y., Zhang S., Zhang J., Study of mechanism of counter-rotating turbine increasing two-stage turbine system efficiency. International Journal of Fluid Machinery and Systems, 2013, 6: 160–169.

[19] Liu Y.B., Zhuge W.L., Zhang Y.J., Zhang S.Y., Numerical analysis of flow interaction of turbine system in two-stage turbocharger of internal combustion engine. IOP Conference Series: Materials Science and Engineering, 2016, 129: 012004.
DOI: 10.1088/1757-899x/129/1/012004.

[20] Hellstrom F., Fuchs L., Numerical computation of the pulsatile flow in a turbocharger with realistic inflow conditions from an exhaust manifold. ASME Turbo Expo 2009: Power for Land, Sea, and Air: American Society of Mechanical Engineers, Orlando, 2009, 6: 8–12.
DOI: GT2009-59619.

[21] Kalpakli A., Örlü R., Tillmark N., Alfredsson P.H., Experimental investigation on the effect of pulsations on exhaust manifold-related flows aiming at improved efficiency. 10th International Conference on Turbochargers and Turbocharging, London, 2012, 5: 15–16.

[22] Lim S.M., Dahlkild A., Mihaescu M., Influence of upstream exhaust manifold on pulsatile turbocharger turbine performance. Journal of Engineering for Gas Turbines and Power, 2019, 141: 061010.

[23] Ding Z., Zhuge W., Zhang Y., Assessment of turbine performance under swirling inflow conditions. Energy, 2019, 168: 492–504.

[24] Ding Z., Zhuge W., Zhang Y., Chen Y., Liu C., Investigation on unsteady and steady swirling inflow effect on turbocharger turbine performance. ASME Turbo Expo 2019: Turbomachinery Technical Conference and Exposition, 2019. DOI: 10.1115/GT2019-91155.

[25] Jeong J., Hussain F., On the identification of a vortex. Journal of Fluid Mechanics, 1995, 285: 69–94.

[26] Futral S.M., Wasserbauer C.A., Off-design performance prediction with experimental verification for a radial-inflow turbine. National Aeronautics and Space Administration, 1965, pp.1–29.